An *ab Initio* Study of Hydrogen Abstraction from Cluster Models for the Diamond Surface

Ronald C. Brown,[†] Chrstopher J. Cramer,[†,‡] and Jeffrey T. Roberts*[,†]

Department of Chemistry and Supercomputer Institute, University of Minnesota, Minneapolis, Minnesota 55455

Received: June 3, 1997[⊗]

Electronic structure calculations have been performed on hydrogen-terminated carbon clusters. Optimized geometries of increasingly larger clusters were examined in order to obtain clusters that accurately model the 111 and 100 diamond surfaces. The clusters were used to characterize the energetics and transition-state structures for hydrogen abstraction by atomic hydrogen from the two surfaces. For the larger clusters, calculations at the MP2/6-31G*//HF/6-31G* level of theory were performed, and these were corrected on the basis of calculations using higher levels of theory applied to representative smaller clusters. It was determined that the barrier to H-atom abstraction from the 100 surface was 2−3 kcal·mol^{-1} higher than that from the 111 surface. The reaction energy for abstraction was also found to be higher from the 100 surface than from the 111 surface, by 3−5 kcal·mol^{-1}.

I. Introduction

The last several years have witnessed intense worldwide activity in the chemical vapor deposition (CVD) of diamond from simple, gaseous hydrocarbon precursors.[1,2] The literature of diamond CVD is now extensive, and reviews have appeared on various aspects of the subject.[3] Numerous kinetic models have been developed to account for diamond growth,[4−6] the most successful of which are based upon Harris's growth-by-methyl mechanism.[7] For reasons having to do with the extreme conditions in a diamond CVD reactor, there are very few rate measurements of the elementary steps leading to diamond growth. Rather, the rate constants in the diamond growth models are generally based upon analogies to gas-phase hydrocarbon reactions. Despite the paucity of experimental rate data, the best of the diamond growth models are amazingly successful at predicting linear growth rates over a wide variety of experimental conditions.[4]

The ability of the kinetic models to predict linear growth rates strongly suggests that they adequately account for the most important chemical reactions involved in diamond CVD. Nevertheless, certain aspects of growth remain poorly understood. For instance, the kinetic models are based upon growth on an idealized 100 diamond surface, or C_d(100). Surfaces other than C_d(100) must also be active for diamond growth, however, since scanning electron microscopy (SEM) images of different diamond films show a wide range of morphologies, with crystallites that terminate in both the C_d(100) and C_d(111) crystal planes.[8] From a technological perspective, this is a critical issue, since the quality and morphology of a diamond film are closely connected. It is not immediately clear how extant kinetic models might be modified to account for morphology, because C_d(100) is the only low Miller index plane of diamond for which one can write a plausible and simple pathway for carbon incorporation into the bulk lattice. Clearly, though, morphology must be related, at least in part, to different chemical properties of different diamond surfaces.

Theory is likely to play a critical role in the development of a molecular-level understanding of diamond CVD, including the origin of morphology, especially given the technical difficulties associated with experimental mechanistic studies. A variety of theoretical methods have been used to study diamond and its growth mechanism, among them *ab initio* molecular orbital calculations[9−11] and molecular dynamics simulations of finite carbon clusters[12−14] and quantum calculations of infinite, periodic carbon slabs.[15,16] For certain problems, such as those involving lattice structure, the latter approach is probably superior. However, when considering chemical reactions at surface sites, such approaches are often less attractive than ones based on clusters because of the lower periodicity of the system.[17]

Various approaches have been used in the investigation of carbon clusters as models for the diamond surface. Small clusters can be treated at high levels quantum mechanically. Moreover, reaction transition states can be identified and characterized with respect to their structures and energies. Much work has therefore concentrated on *ab initio* studies of clusters containing between 9 and 20 carbon atoms.[9−11] The problems that arise from small cluster approaches are generally associated with neglect of the surrounding lattice. Thus, other studies have applied semiempirical quantum schemes to larger clusters.[18−20] Recent studies have combined the *ab initio* and semiempirical approaches, through investigation of a two-region cluster: a small region, containing the reaction sites, is calculated at the *ab initio* level, and a larger region, representing the surrounding lattice, is treated semiempirically.[21,22] A related approach has combined *ab initio* theory with molecular mechanics.[23] The *ab initio*/semiempirical and *ab initio*/molecular mechanics approaches yield results that appear to compare well with experiment. However, their limitations remain to be fully explored.

Here we report a quantum chemical investigation of what is generally acknowledged to be one of the key steps in diamond CVD, abstraction of hydrogen from the diamond surface by atomic hydrogen. On a stable diamond surface, the surface carbon atoms all have covalent bonds to hydrogen, so as to maintain their sp^3 character.[15] The abstraction reaction may thus be written:

$$C_d{-}H + H\bullet_{(g)} \rightarrow C_d\bullet + H_{2(g)} \qquad (1)$$

where C_d−H indicates the hydrogen-terminated diamond surface and C_d• designates a surface from which hydrogen has been

* To whom correspondence should be addressed. Tel: (612) 625-2363. Fax: (612) 626-7541. Internet: roberts@chem.umn.edu.
† Department of Chemistry.
‡ Supercomputer Institute.
⊗ Abstract published in *Advance ACS Abstracts,* October 15, 1997.

S1089-5647(97)01804-X CCC: $14.00

abstracted. Calculations were carried out on clusters of 46 and 35 carbon atoms, designed to model the 111 and 100 surfaces, respectively. To our knowledge, a comparison of the energetics of abstraction from these two surfaces with carefully designed clusters of this size has not been the subject of any previous study. The levels of theory used, HF/6-31G* optimizations and MP2 single-point energy calculations with higher levels performed on small clusters, constitute a realistic quantum mechanical treatment for diamond-like clusters of this size. The work presented herein differs from the combined *ab initio*/semiempirical and *ab initio*/molecular mechanics studies described above in that the entire clusters are treated in a first principles quantum chemical fashion. The clusters are designed to be as large as possible while remaining computationally feasible.

II. Computational Methods

Geometry optimizations for all clusters were carried out at the Hartree−Fock (HF) level of theory using both the STO-3G[24,25] and 6-31G*[26−28] basis sets. For the larger clusters, certain degrees of freedom were held fixed, as discussed in more detail in the next section. Unrestricted Hartree−Fock (UHF) theory was employed for open-shell species. Single-point energies were calculated using perturbation theory truncated at second order (MP2). For H_2 and the 4- and 9-carbon clusters and their corresponding radicals and transition-state structures for hydrogen atom abstraction, the geometries were further optimized at the (U)MP2 level, and zero-point vibrational corrections to the electronic energies were calculated from analytic vibrational frequencies computed at the HF/6-31G* level.

The effects of an incomplete basis set and electron correlation were estimated by single-point energy calculations using the 6−31G*,[26−28] 6−31G**,[26−28] and 6-311G*[29] basis sets at the coupled cluster level of theory including all single, double, and perturbative triple excitations (CCSD(T)).[30,31] To refine the calculations for the larger clusters (where the theory was limited to the MP2/6-31G*//HF/6-31G* level), we define a correction factor based on the smaller clusters according to eq 2. The equation systematically corrects the energies through the inclusion of (i) geometry optimizations at a correlated level of theory, (ii) methods that more completely account for electron correlation, (iii) polarization functions on hydrogen, (iv) basis sets with a valence space expanded to triple-ζ, and (v) zero-point vibrational corrections (ZPVE).

$$\begin{aligned} E(\mathrm{C}) = {} & E(\mathrm{MP2/6\text{-}31G^*}) - E(\mathrm{MP2/6\text{-}31G^*//HF/6\text{-}31G^*}) + \\ & E(\mathrm{CCSD(T)/6\text{-}31G^*//MP2/6\text{-}31G^*}) - E(\mathrm{MP2/6\text{-}31G^*}) + \\ & E(\mathrm{CCSD(T)/6\text{-}31G^{**}//MP2/6\text{-}31G^*}) - \\ & E(\mathrm{CCSD(T)/6\text{-}31G^*//MP2/6\text{-}31G^*}) + \\ & E(\mathrm{CCSD(T)/6\text{-}311G^*//MP2/6\text{-}31G^*}) - \\ & E(\mathrm{CCSD(T)/6\text{-}31G^*//MP2/6\text{-}31G^*}) + \mathrm{ZPVE} \quad (2) \end{aligned}$$

The small clusters cannot accurately simulate diamond, but because they have the same local geometries as the larger clusters, they can be used to calculate corrections to the relative energies of the larger clusters.

All calculations were carried out with the Gaussian94 suite of electronic structure routines.[32]

III. Results

A. Design of the Diamond Clusters. Idealized models of the $C_d(100)$ and $C_d(111)$ surfaces are shown in parts a and b of Figure 1, respectively. In $C_d(111)$, the surface carbons occupy sites analogous to those in cyclohexane in the chair conformation. The nearest-neighbor C−C distance is 1.545 Å. Each surface carbon is bonded to a single hydrogen atom, and the C−H bond vector is perpendicular to the surface plane. In contrast to $C_d(111)$, the 100 surface of diamond is reconstructed from that which is formed from a simple truncation of the bulk lattice.[33] For the unreconstructed surface to form, every surface carbon would have to be bonded to two hydrogen atoms, the result of which would be a high degree of steric repulsion between the hydrogen atoms on neighboring carbons. Reconstruction occurs via the formation of new carbon−carbon bonds (approximately 1.6 Å bond length) between neighboring atoms. The carbons in these so-called dimer pairs have a single C−H bond, and steric repulsion is greatly reduced. The reconstructed surface consists of rows of dimer pairs, separated by troughs approximately 3.4 Å apart.

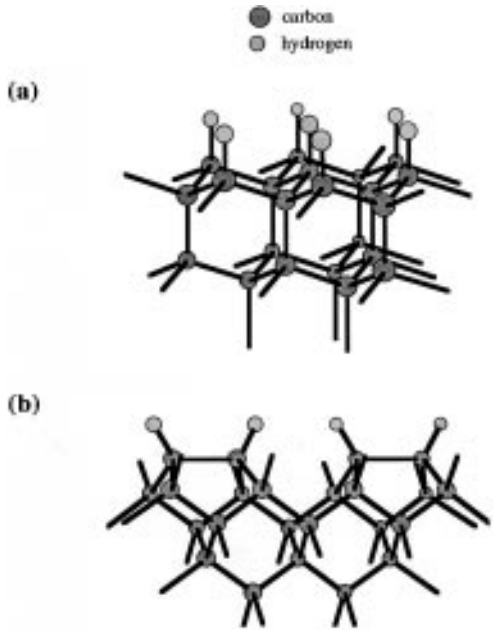

Figure 1. Idealized models of (a) the diamond 111 surface and (b) the reconstructed diamond 100 surface.

The general strategy for cluster design was as follows. First, a number of clusters were identified as potential models for the 111 and 100 surfaces. The structures of the clusters were studied at the HF/STO-3G and HF/6-31G* levels of theory with various degrees of constraint imposed upon the positions of the cluster atoms. The STO-3G basis set was used initially in order to survey geometries efficiently, and the more flexible 6-31G* basis was subsequently used to obtain more accurate results. Constrained atoms were held at fixed positions corresponding to the structure of bulk diamond, while the other atoms were allowed to relax in the geometry optimizations. The final geometries of the optimized structures were examined for convergence with respect to increasing cluster size and degree of constraint. It was assumed that convergence of the cluster geometry around the central site indicated that the significant interactions at that site due to the surrounding lattice had been adequately described.

The $C_d(111)$ clusters, shown in Figure 2, ranged in size from 10 to 70 carbon atoms, and the $C_d(100)$ clusters (Figure 3) had between 9 and 51 carbon atoms. The $C_d(111)$ clusters were all of C_{3v} symmetry, with the principal symmetry axes collinear with the C−H bonds of the central surface carbons. The $C_d(100)$ clusters had C_{2v} symmetry. In the latter clusters, the principal symmetry axes bisect the bonds of the central surface carbon dimers. In the cluster models, it is important to distinguish between the surface and boundary layer carbons.

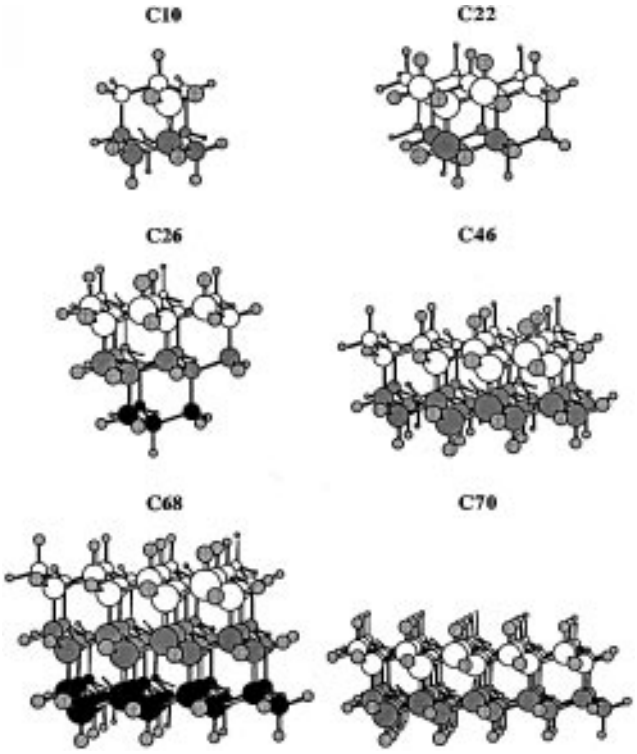

Figure 2. Clusters that were used in the design of the 111 surface cluster. Carbon atoms are represented by solid circles, and the hydrogen atoms are lightly shaded. The first, second, and third-layer carbons are shaded white, gray, and black, respectively.

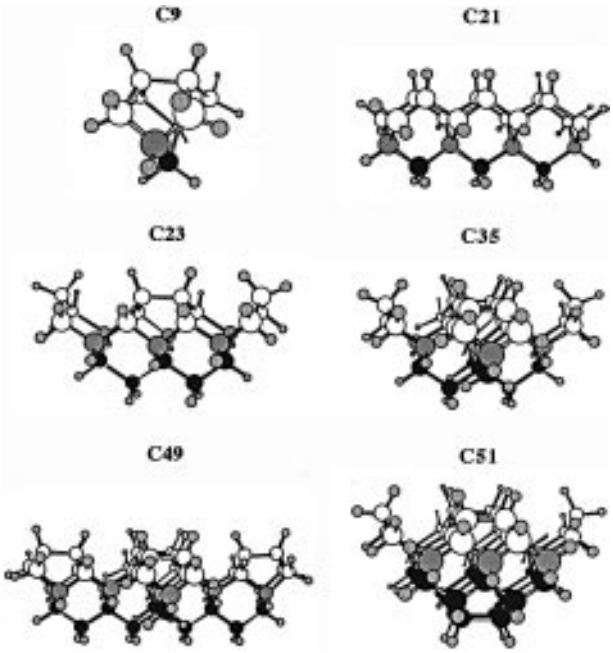

Figure 3. Clusters that were used in the design of the 100 surface cluster. Carbon atoms are solid, while hydrogens are lightly shaded. The top two layers, the third layer, and the fourth layer are shaded white, gray, and black, respectively.

The surface carbons are those in the first layer of carbon atoms; they are the atoms whose reactivity is the subject of this study. The boundary carbons that are below the first layer were terminated with hydrogen to maintain the sp^3 character of the carbon lattice.

In our initial studies, the geometries of the lowest layer carbon atoms were fixed at those found in bulk diamond, i.e., held in perfectly tetrahedral environments with C−C bond lengths of 1.545 Å. This ensures that the models approximate the infinite diamond lattice. The terminating hydrogens on constrained carbons were fixed at a C−H bond length of 1.09 Å. For the three-layer $C_d(111)$ and four-layer $C_d(100)$ clusters, additional calculations were performed that allowed the second and or third layers to relax.

TABLE 1: Calculated Distances between the Central Surface Carbon and the Plane Formed by Its Three Nearest-Neighbors for the $C_d(111)$ Clusters Investigated in This Work[a]

cluster	HF/STO−3G[b]	HF/6−31G*[b]
C10	0.518	0.514
C22	0.498	0.484
C26	0.498 (0.500)	0.483 (0.490)
C46	0.502	0.489
C68	0.502 (0.499)	(0.486)
C70	0.503	

[a] Distances, which are in units of Å, are given for calculations at the HF/STO-3G and HF/6-31G* levels of theory. [b] Results in parentheses are for optimizations relaxing both the top and second layers; all other optimizations relaxed only the top layer.

TABLE 2: Calculated Lengths of the Central Dimer Bonds for the $C_d(100)$ Clusters[a]

cluster	HF/STO-3G[b]	HF/6-31G*[b]
C9	1.581 (1.581)	1.583 (1.583)
C21	1.566 (1.567)	1.570 (1.570)
C23	1.641 (1.606)	1.652 (1.608)
C35	1.627 (1.595)	1.640 (1.598)
C49	1.629 (1.596)	(1.602)
C51	1.624 (1.607)	(1.622)

[a] Distances, which are in units of Å, are given for calculations at the HF/STO-3G and HF/6-31G* levels of theory. [b] Results in parentheses are for three-layer optimizations; all other optimizations relaxed only the top two layers.

In Table 1, we show how one important $C_d(111)$ geometrical parameter, the distance between the central surface carbon and the plane formed by its three nearest carbon atom neighbors, changes with cluster size and degree of constraint. When the number of carbon atoms increases from 46, the distance does not change by more than 0.001 Å at the STO-3G level. When two layers are allowed to relax within the 26- and 68-carbon clusters, the distance changes by as much as 0.007 Å. While not a large effect, this suggests that the local geometry at the surface would be best modeled by allowing for a two-layer optimization. A two-layer optimization was performed on a 68-carbon cluster at the HF/6-31G* level to obtain the positions of carbon atoms for a 46-carbon cluster. This geometry was then truncated to give the 46-carbon cluster that was used for the hydrogen abstraction calculations on a 111 surface.

Some of the results for the 100 surface are summarized in Table 2. The lengths of the central dimer bond in various $C_d(100)$ clusters are shown. The convergence of the dimer bond distance was not as rapid as was observed for the out-of-plane distance with the $C_d(111)$ geometries. This is in part because large clusters are needed to completely include the dimers that lie adjacent to the central dimer. The 35-carbon cluster contains only one of the two carbons on each of the dimers that are across the troughs from the central dimer. An optimization of these carbons without the other half of their dimer pairs would give results that are not consistent with the reconstructed surface. A difference of 0.04 Å in the dimer bond length of the 35-carbon cluster is observed at the HF/6-31G* level when three layers are optimized instead of two. This suggests that deep clusters with three layers being optimized are necessary to approach a consistent dimer bond length.

Several steps were taken to design a cluster that accounts for the effects described above on the central dimer. The first was

TABLE 3: Selected Reactant and Product Geometrical Parameters in Å for (a) the C_d(111) and (b) the C_d(100) Hydrogen Abstraction Reactions

C_d(111)[a]	reactants	products
H1−H2 distance	*b*	0.730
H2−C1 distance	1.092	*b*
C1 to 3-carbon plane distance	0.485	0.392
C_d(100)[c]	reactants	products
H1−H2 distance	*b*	0.730
H2−C1 distance	1.085	*b*
C1−C2 distance	1.621	1.597
C1 to 3-carbon plane distance	0.616	0.545

[a] H1 is the attacking H-atom, and H2 is attached to the surface in the reactants at C1. [b] Infinite separation. [c] H1 is the attacking H-atom, H2 is attached to the surface at C1, and C2 is the carbon dimer atom attached to C1.

a three-layer HF/6-31G* optimization of the 49-carbon cluster that included the full optimization of the adjacent dimers. The positions of the dimer carbons across the trough were then frozen, and the other halves of the dimers were replaced with hydrogen. A three-layer HF/6-31G* optimization with these boundary atoms frozen was then performed on the 51-carbon cluster. This accounted for the effects of the carbons deeper within the lattice. The result was a 35-carbon cluster with all boundary atoms fixed at positions determined by larger optimizations. This cluster is sufficiently small for further study yet contains the appropriate geometry surrounding the central dimer. It was this cluster that was used to study C_d(100) hydrogen abstraction.

B. Hydrogen Abstraction Energetics. Having established that the 46- and 35-carbon atom clusters described above are adequate models for C_d(111) and C_d(100), we proceeded to carry out a theoretical study of the hydrogen abstraction reaction (eq 1). The energies and optimized geometries of the reactants and products were determined at the HF/6-31G* level. The reactants were the hydrogen-terminated diamond cluster and atomic hydrogen. The products consisted of the H_2 molecule and the cluster with a carbon radical at the central site. For the C_d(111) models, the central carbon atom and the 13 carbon atoms closest to it were fully optimized. The rest of the 46 carbons were constrained in their cluster positions determined in the previous section. For the 100 surface, 12 carbon atoms were allowed to relax from their positions in the 35-carbon cluster.

Various aspects of the reactant and product geometries, determined at the HF/6-31G* level, are summarized in Table 3. For both the 111 and 100 surfaces, the reacting carbon atom contracts toward planarity with its three nearest carbon neighbors upon hydrogen abstraction. Partial planarization can be rationalized by hyperconjugation between the p-type orbital on the radical carbon and the sp^3 type bonds on adjacent carbon atoms.[34] From Table 3, it is evident that planarization occurs to a greater extent on the 111 surface. The decreased tendency toward planarity on C_d(100) may be associated with the geometry of the reconstructed surface, the presence of dimer bonds, or the orientation of the C−H bond with respect to the surface plane.

For a more accurate calculation of reactant and product energies, one must include the effects of electron correlation. The 46- and 35-carbon clusters are too large to treat practically at the correlated level. Single-point MP2/6-31G* calculations were performed on clusters that maintained the local site geometries and contained 22 and 27 carbons for the 111 and 100 surfaces, respectively. Further corrections were then made using still higher levels of theory for even smaller clusters, but maintaining appropriate geometries at the reacting carbons. For the 111 surface, the clusters were equivalent to isobutane and its tertiary butyl radical. For C_d(100), the MP2 optimization and the frequency corrections for the closed- and open-shell species were performed with a nine-carbon cluster, while CCSD(T) calculations were done on a four-carbon cluster with C−C bond lengths frozen at the C_d(100) geometry and C−H bond lengths frozen at 1.09 Å. Figure 4 displays the reactant versions of the small clusters that were used to find the corrections. The relative single-point MP2/6-31G* energies of the small clusters followed by the various corrections are shown in Table 4.

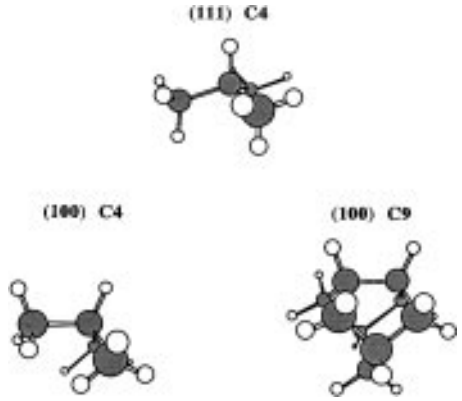

Figure 4. Smallest clusters that preserve the local surface geometry around the central carbon. The optimizations and frequency calculations for the 100 surface used the nine-carbon cluster.

In Table 5, we summarize the energetics of the hydrogen abstraction reaction on the C_d(111) and C_d(100) clusters. It can be seen that the energy difference between products and reactants, after all corrections, is -1.21 kcal·mol^{-1} for reaction at the 111 surface and 2.69 kcal·mol^{-1} for reaction at the 100 surface. It should be pointed out that while there may be significant errors in the *absolute* energies calculated from this level of theory, the *relative* energies of reaction are probably quite accurate, and we consider the comparison between C_d(111) and C_d(100) valid. The C−H bond energy difference of 3.9 kcal·mol^{-1} is likely associated with more complete relaxation into the plane of the radical carbon on the 111 surface. A difference in degree of planar relaxation was also reported recently by Skokov and Frenklach.[22] Their results at the PMP2//UHF/6-31G** level with ZPE corrections showed that the C−H bond strength on C_d(100) exceeds that on C_d(111) by 8.9 kcal·mol^{-1}. The smaller difference calculated herein is likely related to the fact that larger clusters were investigated. From Table 4, it can be shown that the C−H bond energy difference between the four- and nine-carbon clusters is 7 kcal·mol^{-1}, when treated at the single-point MP2 level with ZPE corrections.

C. Transition States to Hydrogen Abstraction. The methods used to determine the transition-state structures and reaction barriers for hydrogen abstraction were similar to those described in the previous section. In particular, the central 13 and 12 carbons and their terminating hydrogens were allowed to relax in the 46- and 35-carbon clusters, respectively. Force constants were examined to verify the existence of a negative frequency along the reaction coordinate, and the energy was maximized with respect to that coordinate while minimized for all other unfrozen degrees of freedom. On the 111 surface, C_{3v} symmetry is maintained because the abstracting hydrogen lies along the same axis as the C−H bond that is being broken. The C_d(100) cluster transition state, on the other hand, relaxes to C_S symmetry. The abstracting hydrogen is again essentially collinear with the dimer carbon and the hydrogen being removed.

A comparison of the two geometries can be found in Table 6. The H−H distance is shorter and the C−H distance is longer

TABLE 4: Relative Energies and Corrections for the Reactants and Products of Hydrogen Abstraction, for the Smallest Representative C_d(111) and C_d(100) Clusters[a]

	111 reactants[b]	111 products	100 reactants[c]	100 products
MP2/6-31G*//HF/6-31G*	0.00	3.74	0.00	9.80
MP2/6-31G* − MP2/6-31G*//HF/6-31G*[d]	0.00	−0.05	0.00	−0.02
CCSD(T)/6−31G*//MP2/6-31G* − MP2/6-31G*[e]	0.00	−4.88	0.00	−4.62
CCSD(T)/6−31G**//MP2/6-31G* − CCSD(T)/6-31G*//MP2/6-31G*[f]	0.00	−2.65	0.00	−3.06
CCSD(T)/6−311G*//MP2/6-31G* − CCSD(T)/6-31G*//MP2/6-31G*[g]	0.00	1.19	0.00	0.68
ZPVE (6−31G*)[h]	0.00	−3.11	0.00	−2.08
total corrections, *E*(C)	0.00	−9.50	0.00	−9.10

[a] Clusters and corrections are described in the text. Energies are given in units of kcal·mol^{-1}. [b] The calculated absolute energies (au) of the reactants at the corresponding levels of theory are −158.326 42 (MP2/6-31G*//HF/6-31G*), −158.326 97 (MP2/6-31G*), −158.398 46 (CCSD(T)/6-31G*//MP2/6-31G*), −158.483 53 (CCSD(T)/6-31G**//MP2/6-31G*), −158.464 72 (CCSD(T)/6-311G*//MP2/6-31G*), 0.140 77 (ZPVE/6-31G*). [c] The calculated absolute energies (au) of the reactants at the corresponding levels of theory are −350.644 19 (MP2/6-31G*//HF/6-31G* C9 cluster), −158.292 48 (MP2/ 6-31G* C4 cluster single-point from C9 geometry), −350.645 16 (MP2/6-31G* C9 cluster), −158.364 33 (CCSD(T)/6-31G*//MP2/6-31G*), −158.450 33 (CCSD(T)/6-31G**//MP2/6-31G*), −158.431 01 (CCSD(T)/6-311G*//MP2/6-31G*), 0.229 60 (ZPVE/6-31G* C9 cluster). [d] This accounts for the term on the first line of eq 2. [e] This accounts for the term on the second line of eq 2. [f] This accounts for the term on the third and fourth lines of eq 2. [g] This accounts for the term on the fifth and sixth lines of eq 2. [h] This accounts for the final term of eq 2.

TABLE 5: Relative Single-Point Energies (in kcal·mol^{-1}) for the Reactants and Products

	MP2/6-31G*//HF/6-31G* reactants[a]	MP2/6−31G*//HF/6-31G* products	product energy after corrections
C_d(111)	0.00	8.29	−1.21
C_d(100)	0.00	11.79	2.69

[a] The calculated absolute energies (au) for the C_d(111) and C_d(100) reactants are 852.881 73 (C22 cluster) and −1046.294 02 (C27 cluster), respectively.

TABLE 6: Selected Bond Lengths and Out-of-Plane Distances in Å and Umbrella Angles in deg for the C_d(111) and C_d(100) Hydrogen Abstraction Transition-State Structures

C_d(111)[a]	transition-state structure
H1−H2 distance	0.949
H2−C1 distance	1.367
C1 to 3-carbon plane distance	0.430
umbrella angle[b]	73.6

C_d(100)[c]	transition-state structure
H1−H2 distance	0.926
H2−C1 distance	1.380
C1−C2 distance	1.604
C1 to 3-carbon plane distance	0.568
umbrella angle	69.3 (dimer) 68.3 (other adjacent C)

[a] H1 is the attacking H-atom, and H2 is attached to the surface in the reactants at C1. [b] Angle between C1−C bonds and line through C1 normal to plane defined by the three substituent atoms. [c] H1 is the attacking H-atom, H2 is attached to the surface at C1, and C2 is the carbon dimer atom attached to C1.

in the C_d(100) transition state than in the C_d(111) transition state. This indicates that the transition state occurs later in the abstraction process on the 100 surface, as expected from the Hammond postulate[35] given the relative endoergicities of the two reactions. The greater degree of planar relaxation of the central carbon on the 111 surface is evident in the transition-state structures just as it was in the products. This is shown by the shorter distance to the nearest-neighbor three-carbon plane and by the umbrella angle. The umbrella angle is defined as the angle between the substituent C−C bonds and the line through the central carbon normal to the three-carbon plane. The structure approaches planarity as the umbrella angle approaches 90°.

The determination of abstraction barrier heights proceeded according to the methodology used for calculation of reaction energies. The single point MP2/6-31G* energies were found using 22- and 27-carbon atom clusters with the geometries taken from the HF/6-31G* optimizations on larger clusters. Additional calculations using the four- and nine-carbon clusters were performed to obtain further corrections. The largest of these corrections, which are listed in Table 7, derive from the coupled cluster calculations. This suggests that there is a moderate degree of multiconfigurational character to the wave functions of these transition states. The barrier for hydrogen abstraction from isobutane, found by applying the total correction *E*(C) to the MP2/6-31G*//HF/6-31G* energy in Table 7, was calculated to be 8.26 kcal·mol^{-1}. The value agrees acceptably with the 7.3 kcal·mol^{-1} CASSCF barrier reported by Page and Brenner[34] and the 6.5 kcal·mol^{-1} barrier used in the rate expression reported by Krasnoperov and co-workers.[36] This agreement suggests that to the extent the transition-state structures are characterized by multiconfigurational wave functions, the CCSD(T) methodology is capable of accurately treating the correlation energetics.

The addition of polarization functions on the hydrogen atoms also gives large corrections to the transition-state energies. It is expected that increased flexibility in the basis set for those hydrogen atoms involved in the abstraction will lead to an improved description of the partial bonding in the transition-state structures. The use of a triple-ζ valence basis set (6-311G*) did not have as large of an effect. It is also evident from Table 7 that the magnitudes of the corrections for the 111 and 100 surfaces are similar. The final values of these activation energies as well as the reaction energies were determined by applying all corrections to the MP2/6-31G* single-point energies. The MP2/6-31G* and the corrected results are shown in Table 8. At the levels of theory treated, the activation energy for hydrogen abstraction was consistently found to be 2−3 kcal·mol^{-1} higher on C_d(100) than on C_d(111).

A contributing factor in the discrepancy of the barrier height is the degree of relaxation of the central carbon atom.[22,34] We believe this to be the same effect that is responsible for the observed difference in reaction energy. To investigate this effect further, a series of calculations was performed in which the umbrella angle of the four-carbon cluster was fixed. The HF/6-31G* transition-state energy at each umbrella angle was determined. Figure 5 is a plot of the hydrogen abstraction transition-state energies, relative to the energy of the fully optimized cluster, as a function of umbrella angle. The optimized umbrella angles from the C_d(100) and C_d(111) carbon clusters are given with the figure. The significant result is that

TABLE 7: Relative Energies and Corrections for the Reactants and Transition-States of Hydrogen Abstraction, for the Smallest Representative C_d(111) and C_d(100) Clusters[a]

	111 reactants[b]	111 transition-state structure	100 reactants[c]	100 transition-state structure
MP2/6-31G*//HF/6-31G*	0.00	18.16	0.00	21.21
MP2/6-31G* − MP2/6-31G*//HF/6-31G*[d]	0.00	0.24	0.00	0.37
CCSD(T)/6-31G*//MP2/6-31G* − MP2/6-31G*[e]	0.00	−3.86	0.00	−4.08
CCSD(T)/6-31G**//MP2/6-31G* − CCSD(T)/6-31G*//MP2/6-31G*[f]	0.00	−3.62	0.00	−3.87
CCSD(T)/6-311G*//MP2/6-31G* − CCSD(T)/6-31G*//MP2/6-31G*[g]	0.00	−0.66	0.00	−0.30
ZPVE (6−31G*)[h]	0.00	−2.00	0.00	−1.90
total corrections, *E*(C)	0.00	−9.90	0.00	−9.78

[a] Clusters and corrections are described in the text. Energies are given in units of kcal·mol^{-1}. [b] The calculated absolute energies (a.u.) of the reactants at the corresponding levels of theory are given in note *a* of Table 5. [c] The calculated absolute energies (a.u.) of the reactants at the corresponding levels of theory are given in note *b* of Table 5. [d] This accounts for the term on the first line of eq 2. [e] This accounts for the term on the second line of eq 2. [f] This accounts for the term on the third and fourth lines of eq 2. [g] This accounts for the term on the fifth and sixth lines of eq 2. [h] This accounts for the final term of eq 2.

TABLE 8: Relative Single-Point Energies (in kcal·mol^{-1}) of the Reactants and Transition-State Structures

	MP2/6-31G*// HF/6-31G* reactants[a]	MP2/6−31G*// HF/6-31G* transition-state structure	transition-state structure energy after corrections
C_d(111)	0.00	18.20	8.30
C_d(100)	0.00	20.81	11.03

[a] The calculated absolute energies (au) of the reactants at the corresponding levels of theory are given in note *a* of Table 6.

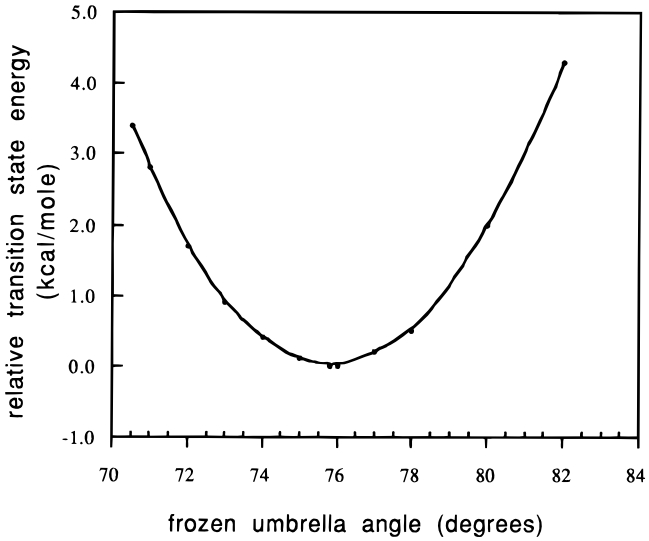

Figure 5. Plot of the relative transition-state energy from a four-carbon cluster vs the frozen umbrella angle. The minimum occurs at 75.82°, while the tetrahedral arrangement has an umbrella angle of 70.53°. The C_d(111) transition state was found to occur when the umbrella angle was 73.6° and the C_d(100) transition state had umbrella angles of 69.3° and 68.3° with the dimer and the other adjacent carbons, respectively.

the umbrella angle present in the C_d(111) transition state is closer to the value that gives the minimum energy. While an investigation of the reactants and products would likely show a similar trend, the fact that the C_d(100) transition state does not attain as much of the available relaxation energy as the C_d(111) transition state contributes to the larger barrier.

IV. Conclusion

An important goal of this study was the design of clusters that accurately model the 111 and 100 diamond surfaces at a local site and that could be treated at a high level of *ab initio* theory. Due to the careful treatment of considerations such as cluster size and degree of optimization, we are confident that the 46- and 35-carbon clusters give accurate geometries for the local sites and constrained boundary atoms.

A comparison of hydrogen abstraction energetics from the 100 and 111 surfaces has not previously been done with clusters of this size at this level of theory. Smaller clusters were necessary when electron correlation and higher levels of theory were considered. For this reason inaccuracies may still be present in the resulting energies. However, similar differences between the surfaces were observed at every level of theory. We conclude that the barrier to hydrogen abstraction from the 100 surface is 2−3 kcal·mol^{-1} higher than from the 111 surface. The hydrogen being abstracted is closer to the abstracting hydrogen and further from the carbon in the C_d(100) transition state than in the C_d(111) transition state. This suggests that in addition to having a larger relative energy, the C_d(100) transition state is closer in geometry to the products (the H_2 molecule and the radical carbon on the diamond surface) than the C_d(111) transition state. Although other effects may be present, it is clear that the more incomplete relaxation of the C_d(100) dimer carbon toward planarity is a factor in these differences.

Acknowledgment. The support of the Minnesota Supercomputer Institute is gratefully acknowledged.

References and Notes

(1) Angus, J. C.; Hayman, C. C. *Science* **1988**, *241*, 913.
(2) Yarbrough, W. A.; Messier, R. *Science* **1990**, *247*, 688.
(3) See, for example: Spear, K. E., Dismukes, J. P., Eds. *Synthetic Diamond*: *Emerging CVD Science and Technology*; Wiley: New York, 1994.
(4) Wu, B. W.; Girshick, S. L. *J. Appl. Phys.* **1994**, *75*, 3914.
(5) Goodwin, D. G. *Appl. Phys. Lett.* **1991**, *59*, 277.
(6) Harris, S. J.; Goodwin, D. G. *J. Phys. Chem.* **1993**, *97*, 23.
(7) Harris, S. J. *Appl. Phys. Lett.* **1990**, *56*, 2298.
(8) Busmann, H. G.; Zimmerman-Edling, W.; Sprang, H.; Guntherodt, H. J.; Hertel, I. V. *Diamond Relat. Mater.* **1992**, *1*, 979.
(9) Hukka, T. I.; Pakkanen, T. A.; D'Evelyn, M. P. *J. Phys. Chem.* **1995**, *99*, 4710.
(10) Larsson, K.; Carlsson, J. O.; Lunell, S. *Phys. Rev. B* **1995**, *51*, 10003.
(11) Latham, C. D; Heggie, M. I. *Diamond Relat. Mater.* **1993**, *2*, 1493.
(12) Song, K.; de Sainte Claire, P.; Hase, W. L. *Phys. Rev. B* **1995**, *52*, 2949.
(13) Garrison, B. J.; Dawnkaski, E. J.; Srivastava, D.; Brenner, D. W. *Science* **1992**, *255*, 835.
(14) Alfonso, D.; Drabold, D.; Ulloa, S.; *J. Phys.*: *Condens. Matter* **1996**, *8*, 641.
(15) Davidson, B. N.; Pickett, W. E. *Phys. Rev. B* **1994**, *49*, 11253.
(16) Kress, C.; Fiedler, M.; Schmidt, W. G.; Bechstedt, F. *Surf. Sci.* **1995**, *331*−333, 1152.
(17) Sauer, J. *Chem. Rev. (Washington, D.C.)* **1989**, *89*, 199.
(18) Huang, D.; Frenklach, M. *J. Phys. Chem.* **1991**, *95*, 3692.
(19) Huang, D.; Frenklach, M. *J. Phys. Chem.* **1992**, *96*, 1868.
(20) Skokov, S.; Weiner, B.; Frenklach, M. *J. Phys. Chem.* **1994**, *98*, 7073.
(21) Skokov, S.; Weiner, B.; Frenklach, M. *Phys. Rev. B* **1997**, *55*, 1895.
(22) Frenklach, M.; Skokov, S. *J. Phys. Chem. B* **1997**, *101*, 3025.

(23) Musgrave, C. B.; Harris, S. J.; Goddard, W. A. *Chem. Phys. Lett.* **1995**, *247*, 359.
(24) Hehre, W. H.; Stewart, R. F.; Pople, J. A. *J. Chem. Phys.* **1969**, *51*, 2657.
(25) Hehre, W. J.; Ditchfield, R.; Stewart, R. F.; Pople, J. A. *J. Chem. Phys.* **1970**, *52*, 2769.
(26) Ditchfield, R.; Hehre, W. J.; Pople, J. A. *J. Chem. Phys.* **1971**, *54*, 724.
(27) Hehre, W. J.; Ditchfield, R.; Pople, J. A. *J. Chem. Phys.* **1972**, *56*, 2257.
(28) Hariharan, P. C.; Pople, J. A. *Chem. Phys. Lett.* **1972**, *66*, 217.
(29) Krishnan, R.; Binkley, J. S.; Seeger, R.; Pople, J. A. *J. Chem. Phys.* **1980**, *72*, 650.
(30) Cizek, J. *Adv. Chem. Phys.* **1969**, *14*, 35.
(31) Purvis, G. D.; Bartlett, R. J. *J. Chem. Phys.* **1982**, *76*, 1910.
(32) Frisch, M. J.; Trucks, G. W.; Schlegel, H. B.; Gill, P. M. W.; Johnson, B. G.; Robb, M. A.; Cheeseman, J. R.; Keith, T.; Petersson, G. A.; Montgomery, J. A.; Raghavachari, K.; Al-Laham, M. A.; Zakrzewski, V. G.; Ortiz, J. V.; Foresman, J. B.; Cioslowski, J.; Stefanov, B. B.; Nanayakkara, A.; Challacombe, M.; Peng, C. Y.; Ayala, P. Y.; Chen, W.; Wong, M. W.; Andres, J. L.; Replogle, E. S.; Gomperts, R.; Martin, R. L.; Fox, D. J.; Binkley, J. S.; Defrees, D. J.; Baker, J.; Stewart, J. P.; Head-Gordon, M.; Gonzalez, C.; Pople, J. A. *Gaussian 94, Rev. D.1*; Gaussian Inc.: Pittsburgh, PA, 1995.
(33) Skokov, S.; Weiner, B.; Frenklach, M. *J. Chem. Phys.* **1995**, *102*, 5486.
(34) Page, M.; Brenner, D. W. *J. Am. Chem. Soc.* **1991**, *113*, 3270.
(35) Hammond, G. S. *J. Am. Chem. Soc.* **1955**, *77*, 334.
(36) Krasnoperov, L. N.; Kalinovski, I. J.; Chu, H.; Gutman, D. *J. Phys. Chem.* **1993**, *97*, 11787.